DESIGN OF AN ACTIVE FILTER FOR FUEL CELL SYSTEMS

Yales Rômulo de Novaes and Ivo Barbi
Power Electronics Institute - INEP
Federal University of Santa Catarina - UFSC
88040-970 – Florianópolis - SC - Brazil
P.O. Box: 5119 - +55-48-331-9204
www.inep.ufsc.br
yales@inep.ufsc.br - ivobarbi@inep.ufsc.br

Abstract – This paper presents an active filter connected into a fuel cell power conditioning system to suppress the low frequency ripple current produced by single-phase inverters. Effects, control strategies and design procedure were presented.

KEYWORDS

Fuel Cells, Converter, Active Filter, Ripple, bi-directional.

SYMBOLS

Po_{inv}	Inverter output power
Vp	Inverter output peak voltage
Ip	Inverter output peak current
Vo	Inverter output voltage
ω	Angular freq. of the output voltage of the inverter/ripple current
Ii_{inv}	Inverter input current
Io_{conv}	DC-DC converter output current
Vo_{conv}	DC-DC converter output voltage
η	Efficiency
Mi	Modulation index
PF	Power factor
PI_{conv}	DC-DC active power input
SI_{conv}	Volt-ampere power (rms values)
H_R	Reactive power (harmonics)
IZfc	Fuel cell ripple current
IZbat	Battery ripple current
Zbat	Baterry impedance
Zfc	Fuel cell impedance
D	DC-DC converter duty cycle
n	DC-DC transformer turns ratio
ZCo	DC-DC converter output capacitor impedance
ZCi	DC-DC converter input capacitor impedance
ZLi	DC-DC converter input inductor impedance
ZLo	DC-DC converter input inductor impedance
Ib	Ripple current caused by the DC-AC conversion
VCf	Capacitor Cf voltage
Vb	Battery/fuel cell voltage
Ip	Inductor ILf peak current

I. INTRODUCTION

Fuel cells (FC) are devices that convert chemical energy directly into electrical energy without any intermediary processes, differing from combustion engines that need to convert chemical energy into thermal energy, then into electrical energy, and have their efficiency limited by the Carnot Cycle [1]. Fuel cells have potential to supply electrical energy while being supplied with reactants, like hydrogen and oxygen, making them a very interesting technology to help substitute oil for other less pollutants fuels. An interesting fuel for our country and others is the sugar-cane alcohol, that is rich in hydrocarbons, which can be converted into hydrogen using a fuel reformer. The biggest advantage of this fuel is that the CO_2 generated by the reformer processes will be consumed by sugar-cane plantation during the next crop. Of course, the emissions produced and the energy consumed by fermentation and agricultural machines need to be taken into account.

Like other electrical generators, fuel cells have some particular characteristics or electrical requirements that need to be respected when a power processing system is to be designed. One of them is the ripple current parameter. For the efficient operation of a fuel cell, the hydrogen flow needs to be adjusted to the electrical power consumption, especially when a reformer is being used. The hydrogen flow is directly linked to the electrical current, this is immutable. Since the fuel adjustment is made by mechanical devices, it may be slower than electrical current variations. Figure 1 shows a steady state voltage characteristic of a PEMFC (Proton Exchange Membrane Fuel Cell), for different hydrogen flows. Note that for hydrogen flows smaller than the base flow, the mass transport region occurs at a smaller current value [2,3]. Since the efficiency of a PEMFC is dictated by the relationship between the actual voltage and the open circuit voltage, the energy that is not converted into electrical energy will heat the fuel cell. The operation during long periods of time in the mass transport region needs to be avoided. Large and fast changes in the load current can make difficult the humidification of the fuel cell membrane and the fuel flow control. In some cases a harmful electrochemical reaction can take place. In the same way, large ripple currents need to be avoided, especially at frequencies below 400 Hz [3]. On the other hand, during the start-up of the fuel cell, some energy storage device is needed, depending on which kind of system the fuel cell is being used in.

Motivated by these reasons, this work was performed to show some ways to reduce the ripple current.

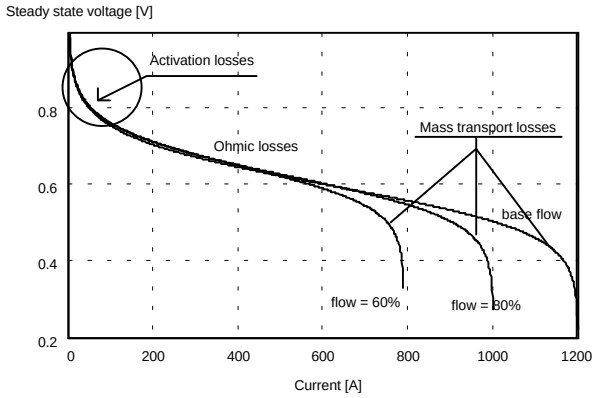

Fig. 1 – Steady state voltage of a PEM fuel cell for different fuel flows.

II. THE RIPPLE CURRENT ORIGIN

Stand-alone AC generation was chosen as the main focus of this paper. However, the solution that will be presented can be extended to other application areas. Inside this context, extensive research was performed in literature [4-13] to find which architectures have been used to process electrical power, also called power conditioning systems.

It is clear that when a load is fed by a single-phase AC-supply, the power processed by the AC-DC and DC-DC converters is pulsed. This phenomenon occurs in both Fuel Cell applications and Uninterruptible Power Supplies (UPS). It can be better understood by taking as an example the simplest architecture, shown in Fig. 2.

The instantaneous power of the output inverter can be expressed as (1) and (2).

$$Po_{inv}(t) = Vp \cdot \sin(\omega \cdot t) \cdot Ip \cdot \sin(\omega \cdot t) \quad (1)$$

$$Po_{inv}(t) = 2 \cdot Vo_{rms} \cdot Io_{rms} \cdot \sin^2(\omega \cdot t) \quad (2)$$

Considering the efficiency and the modulation index, Mi, of the inverter, its input current can be expressed by (3) and the converter output current can be expressed by (4).

$$Ii_{inv}(t) = Io_{conv}(t) = \frac{2 \cdot Vo_{rms} \cdot Io_{rms}}{Vo_{conv} \cdot \eta_{inv}} \cdot \sin^2(\omega \cdot t) \quad (3)$$

$$\frac{Io_{conv}}{Io_{rms}} = \overline{Io_{conv}} = \frac{2\sqrt{2} \cdot Mi}{\eta_{inv}} \cdot \sin^2(\omega \cdot t) \quad (4)$$

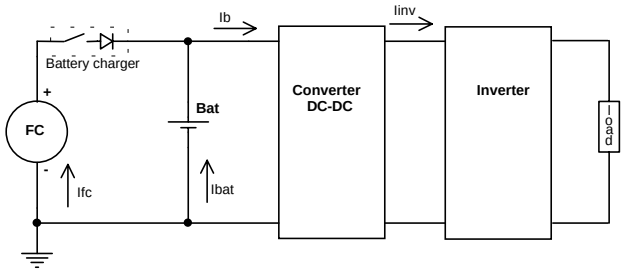

Fig. 2 - Architecture chosen as an example.

Figure 3 shows the instantaneous power drained by the inverter, represented by a DC component and a AC component. The peak power processed by the DC-DC converter is twice the nominal power of the inverter.

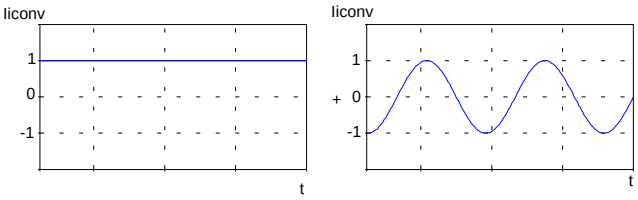

Fig. 3 - DC-DC converter's instantaneous input power.

Considering the FC as an ideal power source, all of this low frequency ripple current will circulate through the FC and the battery. Therefore, the power factor of this system is not unity, and can be calculated using (5) until (9).

$$PF = \frac{P_{Iconv}}{S_{Iconv}} \quad (5)$$

$$PF = \frac{\frac{1}{2\pi}\int_0^{2\pi} 2 \cdot Vo_{rms} \cdot Io_{rms} \cdot \sin^2(\omega t)\, d\omega t}{\sqrt{\frac{1}{2\pi}\cdot\int_0^{2\pi}\left(Vo_{conv}(t)\right)^2 d\omega t}\cdot\sqrt{\frac{1}{2\pi}\int_0^{2\pi}\left(\frac{2 \cdot Vo_{rms} \cdot Io_{rms}}{Vo_{conv}} \cdot \sin^2(\omega t)\right)^2 d\omega t}} \quad (6)$$

$$P_{Iconv} = V_{O_{rms}} \cdot I_{O_{rms}} \quad (7)$$

$$S_{Iconv} = \frac{\sqrt{6}}{2} \cdot V_{O_{rms}} \cdot I_{O_{rms}} \quad (8)$$

$$FP = \frac{\sqrt{6}}{3} = 0{,}816 \quad (9)$$

The reactive power that would circulate through the FC and battery terminals, can be determined by (10) and (11).

$$H_R = \sqrt{Si_{conv}^{\ 2} - Pi_{conv}^{\ 2}} \quad (10)$$

$$H_R = \frac{1}{\sqrt{2}} \cdot P_{Iconv} \quad (11)$$

These calculations can represent an image of the performance of a power conditioning system based on FC's. An observation needs to be made about the DC-DC voltage control. If the DC-DC voltage control loop is designed to eliminate any low frequency disturbance, like 120Hz, the previous calculations are correct. Otherwise, if a low frequency ripple voltage is admitted at the DC-DC output, which can be reduced by the output capacitor, only a part of that ripple current will circulate through the primary and secondary sources. A greater reduction in the FC and battery ripple currents will be noted by taking into consideration the impedances of these sources. A detailed analysis and determination of the distribution of this ripple current are presented in [14]. Here, it will be assumed that (12) until (14) can provide necessary information on current distribution.

$$IZfc = \frac{Zbat}{Zfc + Zbat} \cdot \frac{\frac{Ib \cdot ZCo \cdot n \cdot \sqrt{D} \cdot ZCi}{D^2 \cdot Zx \cdot n^2 + ZLo + ZCo}}{ZLi + ZCi + \frac{Zfc \cdot Zbat}{Zfc + Zbat}} \quad (12)$$

$$IZbat = \frac{Zfc}{Zfc + Zbat} \cdot \frac{\frac{Ib \cdot ZCo \cdot n \cdot \sqrt{D} \cdot ZCi}{D^2 \cdot Zx \cdot n^2 + ZLo + ZCo}}{ZLi + ZCi + \frac{Zfc \cdot Zbat}{Zfc + Zbat}} \quad (13)$$

$$Zx = \frac{\left(\frac{Zfc \cdot Zbat}{Zfc + Zbat} + ZLi\right) \cdot ZCi}{\frac{Zfc \cdot Zbat}{Zfc + Zbat} + ZLi + ZCi} \quad (14)$$

Since large ripple currents are not readily accepted by batteries and especially by Fuel Cells, an active filter can be designed to drain this reactive power. There are other ways to reach this objective, like controlling the current drained by the DC-DC converter or using passive filters.

III. ACTIVE FILTER

A. Topology and architecture

The topology chosen to be the active filter converter is

shown in Fig. 4. This topology is composed of a buck converter to transfer the reactive power from capacitor Cf to the fuel cell power conditioning system, and by a Boost converter to drain the reactive power from the power conditioning system to capacitor Cf.

This active filter can be connected between the inverter and the DC-DC converter. In this configuration, ideally, the power processed by the active filter (reactive power) will have the same value as the active power processed by the inverter, thus, resulting in a bulky active filter. Therefore, blocking the ripple current by using the DC-DC converter maybe be a better solution. But, by using batteries or ultracapacitors (UC's), remembering that UC's support larger ripple currents than batteries, this configuration will be able to supply energy during load variations, during the fuel cell warm-up and filter the ripple current, being very attractive. The main advantage of connecting the active filter in this manner, is that the DC-DC converter will not have low frequency ripple current circulating through the transformer that causing losses. No overdimensiong related to the load variations will be necessary.

To prove the concepts of using an active filter, filtering low frequency currents, in fuel cell systems, this work will show analyses and experimental results of connecting an active filter at the input of a DC-DC converter, as shown in Fig. 5.

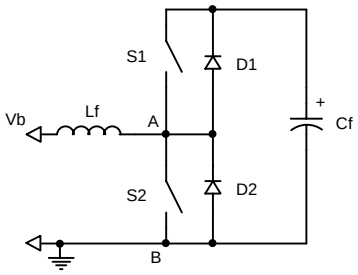

Fig. 4 – Topology of the active filter converter.

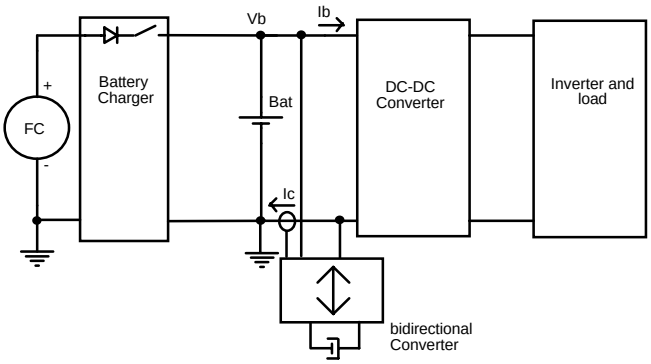

Fig. 5 – Connection point of the active filter in the fuel cell power conditioning system.

B. Control strategy

The voltage across capacitor Cf will be held at a value greater than the input voltage. Considering this voltage constant and controlled, the current of inductor Lf can be imposed. Figure 6 illustrates this situation, where an AC current can be obtained by using an adequate modulation.

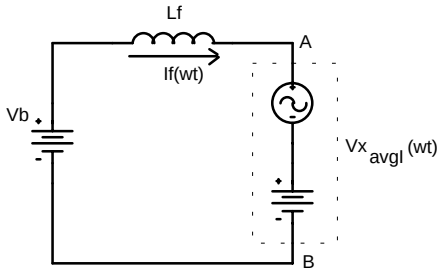

Fig. 6 - Inductor current control.

The voltage generated by the modulation is presented by (15), where ω is twice the output voltage inverter's frequency.

$$VxavgI(\omega t) = Vb - Lf \cdot \omega \cdot Ip \cdot \cos(\omega t) \quad (15)$$

Therefore, the minimal value of the voltage across the capacitor Cf or the maximum value of the inductance Lf, is determined by (16).

$$VCf_{min} > Vb + Lf \cdot \omega \cdot Ip \quad (16)$$

The duty cycle during a modulation period can be determined by (17).

$$D(\omega t) = \beta - \frac{Lf \cdot \omega \cdot Ip \cdot \cos(\omega t)}{VCf} \quad (17)$$

Two strategies to control the active filter are suggested. One of them is calculating a reference current and directly controlling the inductor current. This solution is shown in Fig. 7. This solution seems to be more complicated to be implemented, depending of course, of implementation method (DSP or analog circuits). The advantage is that the inductor current can be easily limited.

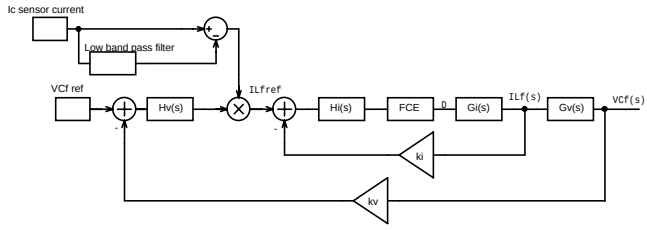

Fig. 7 - Active filter control strategy.

Figure 8 presents the other solution. In this strategy, the current drained from the FC and the battery is controlled by using a constant reference value obtained from the active filter's voltage control loop. Only one precision current sensor has to be used in this strategy, but a current limithing sensor for the active filter is also necessary. This solution was the strategy chosen to be implemented.

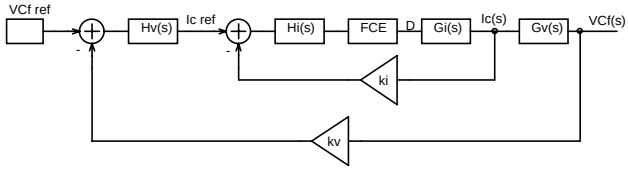

Fig. 8 - Active filter control strategy.

The transfer function of the input current divided by the duty cycle was obtained by the traditional modeling method and is presented as follows. Equations (17) until (25) show

this procedure.

$$Vx_{avg} = \frac{1}{T}\int_{0}^{T(1-D)} VCf\ dt \quad (18)$$

$$Vx_{avg} = VCf \cdot (1-D) \quad (19)$$

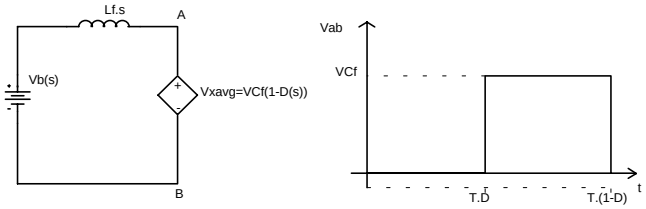

Fig. 9 - Average value of voltage VCf, considering D=1 when S2 is closed (boost operation).

Applying circuit analysis, the current ILf(s) is obtained and presented by (21).

$$-Vb(s) + ILf(s) \cdot s \cdot Lf + VCf(s)(1-D) = 0 \quad (20)$$

$$ILf(s) = \frac{Vb(s)}{s \cdot Lf} - \frac{VCf(1-D)}{s \cdot Lf} \quad (21)$$

Applying a variation in the duty cycle, current ILf will change. Eliminating constant values from (22), the transfer function of the input current divided by the duty clycle is presented in (25).

$$ILf(s) + \Delta ILf(s) = \frac{Vb(s)}{s \cdot Lf} - \frac{VCf\left(1-\left(D(s)+\Delta D(s)\right)\right)}{s \cdot Lf} \quad (22)$$

$$\Delta ILf(s) = -\frac{VCf \cdot \Delta D(s)}{s \cdot Lf} \quad (23)$$

$$ILf(s) = -\frac{VCf \cdot D(s)}{s \cdot Lf} \quad (24)$$

$$\frac{ILf(s)}{D(s)} = -\frac{VCf}{s \cdot Lf} \quad (25)$$

Using similar methods, the voltage transfer function was obtained and is presented in (26).

$$\frac{VCf(s)}{ILf(s)} = \frac{1}{s \cdot Cf} \quad (26)$$

C. Voltage and current stresses

The input current of the active filter will be the sum of (12) and (13), and the peak value of this current will be named Ip.

In order for the active filter to reach symmetrical operation, with an equal distribution of the current between the switches, the voltage VCf needs to be determined by (27).

$$VCf = 2 \cdot Vb \quad (27)$$

Therefore, the voltage across all of the switches is VCf.

Defining a relationship between Vb and VCf:

$$\beta = \frac{Vb}{VCf} \quad (28)$$

Hence, the current stress in the inductor, in the switches and in the Cf capacitors can be calculated by (29) until (38). A graph was created to be used by design engineers, and is presented in the Fig. 10.

$$\overline{ILf_{rms}} = \frac{ILf_{rms}}{Ip} = \frac{1}{\sqrt{2}} \quad (29)$$

$$IS1_{avg} = \frac{1}{2\pi} \cdot \int_{0}^{\pi} Ip \cdot \sin(\omega t) \cdot \left(\beta - \frac{Lf \cdot Ip \cdot \omega}{VCf} \cdot \cos(\omega t)\right) d\omega t \quad (30)$$

$$\overline{IS1_{avg}} = \frac{IS1}{Ip} = \frac{\beta}{\pi} \quad (31)$$

$$IS1_{rms} = \sqrt{\frac{1}{2\pi}\int_{0}^{\pi}\left(Ip \cdot \sin(\omega t) \cdot \sqrt{\beta - \frac{Lf \cdot Ip \cdot \omega}{VCf} \cdot \cos(\omega t)}\right)^2 d\omega t} \quad (32)$$

$$\overline{IS1_{rms}} = \frac{IS1_{rms}}{Ip} = \frac{1}{2} \cdot \sqrt{\beta} \quad (33)$$

Using the same logic, the other stresses can be defined by (33) until (37).

$$\overline{IS2_{avg}} = \frac{1-\beta}{\pi} \quad (34)$$

$$\overline{IS2_{rms}} = \frac{\sqrt{1-\beta}}{2} \quad (35)$$

$$\overline{ID1_{avg}} = \overline{IS1_{avg}} \quad (36)$$

$$\overline{ID2_{avg}} = \overline{IS2_{avg}} \quad (37)$$

$$\overline{ICf_{rms}} = \frac{\sqrt{2 \cdot \beta}}{2} \quad (38)$$

The inductor can be determined using the maximum ripple current admissible at the switching frequency, presented by (39), (39) and (40).

$$Lf = \frac{Vb \cdot (\beta - 1)}{-\Delta ILf \cdot fc + \beta \cdot \omega \cdot Ip} \quad (39)$$

$$\overline{\Delta ILf} = (1+\beta) \cdot (\alpha - 1) \quad (40)$$

Where:

$$\alpha = \frac{Lf \cdot \omega \cdot Ip}{Vb} \quad (41)$$

The minimal value of capacitor Cf can be determined by (42).

$$Cf = \frac{2 \cdot Lf \cdot ICf_{rms}^{\ 2}}{\Delta VCf^{\,2}} \quad (42)$$

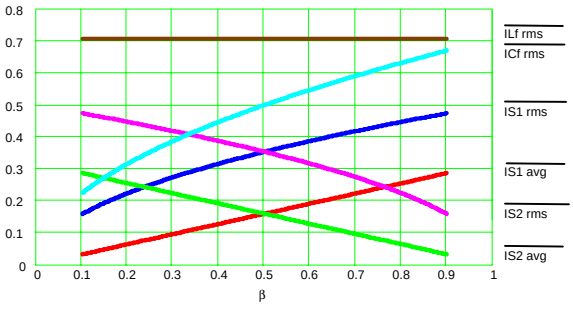

Fig. 10 - Current stress in the active filter components.

D. Filter Design

Using the equations previously presented, the active filter was implemented, making use of the following information.

- Regarding the inductor:

$ILf_{rms} = 11{,}1A$; $Lf = 350\mu H$; $ILf_{peak} = 16A$; $\Delta ILf = 0{,}6A$.

- Fuel cell voltage:

$Vb_{max} = 37V$;

- Regarding the switches:

$IS1_{rms} = IS2_{rms} = 5{,}5A$;

$ID1_{avg} = ID2_{avg} = 2{,}5A$;

MOSFET IRF540N.

- Regarding capacitor Cf:

$ICf_{rms} = 7{,}8A$; $\Delta VCf = 7{,}5V$; $VCf = 75V$; $Cf = 760\mu F$ (Calculated) and $Cf = 3000\mu F$ (implemented).

- Heat sink: natural cooling, thermal resistance equal to 3W/°C.
- Current sensor mark LEM, ref. LAS50TP.
- Switching frequency: 100 kHz.

The control circuit was implemented using the UC3854 but, the multiplier stage is not necessary. Therefore, any other integrated circuit could be used. The switches were gated using the IR2110, with complementary command.

IV. Simulation and Experimental results

Figure 11 shows an example of the ripple current distribution in a FC system supplying a 1kW resistive load.

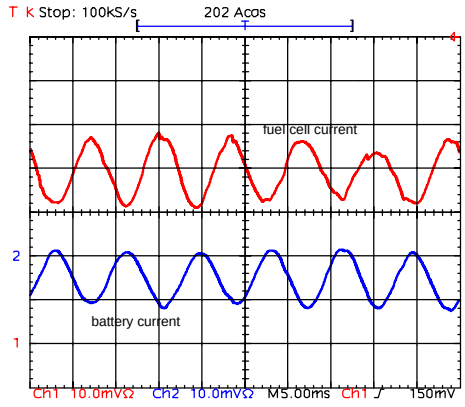

Fig. 11 - Current drained from the Fuel Cell and from a battery, for a 1kW inverter system (10A/div).

The active filter simulation results are presented in Fig. 12. Note that the current of the fuel cell and the battery are free from ripple currents. During a load variation, the active filter takes on this variation and tries to maintain the fuel cell current constant. Therefore, short load variations can be supplied by the energy stored in capacitor Cf. The duration of these variations depends on the voltage control loop of the filter. If the voltage control loop is slow, then the rise or fall of the fuel cell and battery currents will be slower. These results were obtained using models of batteries and fuel cells [15], with convenient parameters to simplify the simulation.

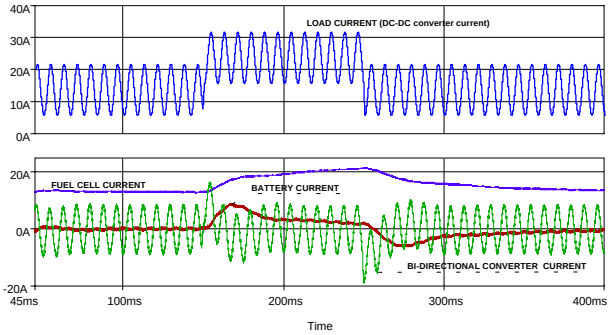

Fig. 12 - Simulation results of the active filter in a fuel cell system during a load variation.

The experimental results are presented as follows. Figure 13 presents the current drained by the converters (Ib), the current drained by the active filter (ILf) and voltage VCf. Figure 14 presents the current drained by the fuel cell/batteries and current Ic. Note that a significant reduction in the ripple current was reached. The high frequency ripple current is presented in Fig. 15.

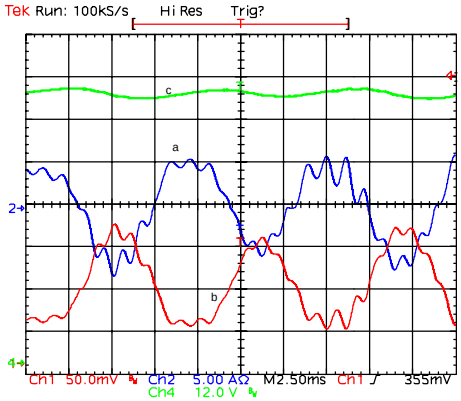

Fig. 13 - Active filter - (a) Current ILf; (b) Current Ib (10mV/A), (c) Voltage VCf.

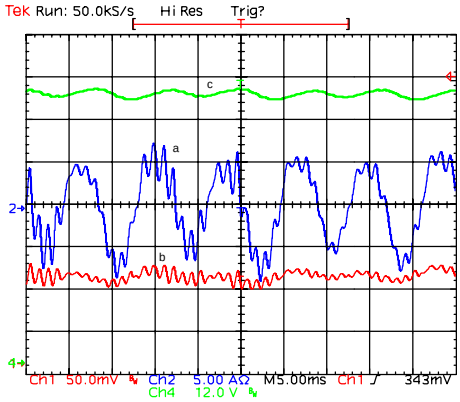

Fig. 14 - Active filter - (a) Current ILf (10mV/A); (b) Current Ic, (c) Voltage VCf.

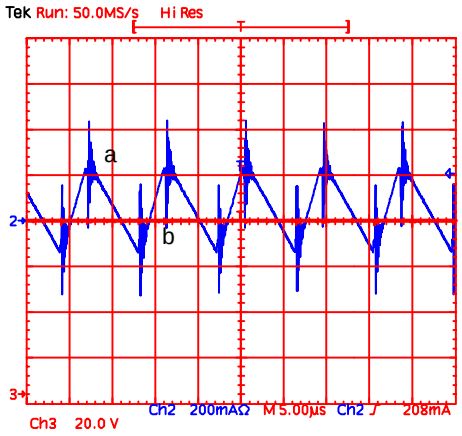

Fig. 15 - Active filter - current ILf and voltage VCf.

Figure 13 presents a picture of the prototype. Inductor Lf was made using a toroid core. The relationship between the input reactive power and the volume is presented by (43) and the relationship between the reactive power and the weight is shown by (44).

$$Ve = 0.23\frac{VA}{cm^3} \tag{43}$$

$$Me = 320\frac{VA}{kg} \tag{44}$$

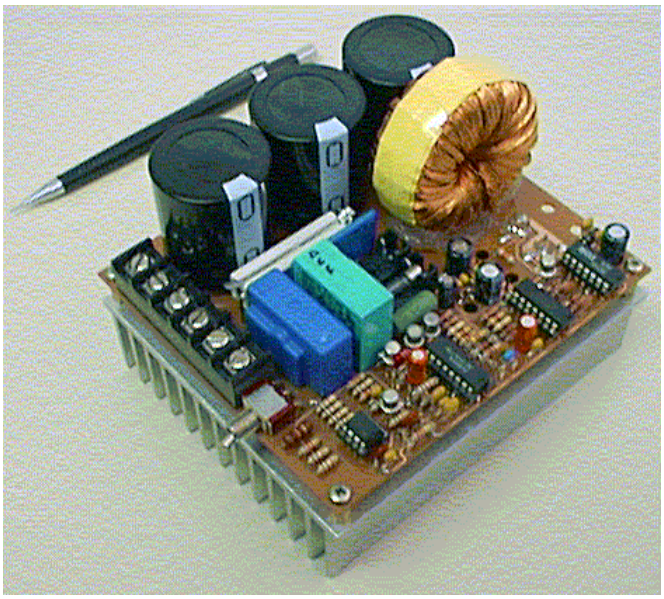

Fig. 16 - Picture of the implemented prototype.

V. CONCLUSION

An active filter was designed to reduce the low frequency ripple current in a fuel cell system. Information regarding the origin of this ripple current, effects in fuel cell systems, control strategies and a design procedure were presented. The behavior during load variations was also discussed.

ACKNOWLEDGEMENTS

The authors gratefully acknowledge PHB Electronic Ltd for the fuel cell system equipment and financial support.

We would like to thank LEM S/A and Intech Engineer Ltd, especially J. E. Antonio, for the Hall effect sensors supplied.

REFERENCES

[1] LARMINIE, James; DICKS, Andrew. Fuel Cell Systems Explained. Editora: John Wiley & Sons, 2000.

[2] P.T. Krein, "Fuel Cells : Electrical Energy Conversion Issues", Power Point presentation of the University of Illinois at Urbana-Champaign, nov 2002.

[3] R.S. Gemmen, "Analysis for the Effect of Inverter R ipple Current on Fuel Cell Operating Condition" at www.energychallenge.org, nov. 2001.

[4] E. Santi, et al., "A Fuel Cell Based Domestic Uninterruptible Power Supply", in Proc IEEE Applied Power Electronics Conf., 2002, pp. 605-613.

[5] T.A. Nergaard, et al "Design Considerations for a 48V Fuel Cell to Split Single Phase Inverter System with Ultracapacitor Energy Storage", in Proc IEEE Power Electronics Specialist Conf., 2002, pp. 257-261.

[6] A.M. Tuckey, J.N. Krase, "A Low-Cost Inverter for Domestic Fuel Cell Applications", in Proc. IEEE Power Electronics Specialist Conf., 2002, pp

[7] R. Gopinath, et al., "Development of a Low Cost Fuel Cell Inverter System with DSP Control", in Proc. IEEE Power Electronics Specialist Conf., 2002, pp. 309-314.

[8] A. Monti et al., "Fuel Cell Based Domestic Power Supply - A Student Projetc", in Proc. IEEE Power Electronics Specialist Conf., 2002, pp. ??

[9] K. Wang et al., "Bi-directional DC to DC Converters for Fuel Cell Systems", in Proc. IEEE Power Electronics Specialist Conf. 2002, pp. 47-51,

[10]A.D. Napoli, et al., "Multiple Input DC-DC Power Converter for Fuel-Cell Powered Hybrid Vehicles", in Proc IEEE Power Electronics Specilist Conf., 2002, pp. 1685-1690.

[11]C. Liu et al., "Power Balance Control and Voltage Conditioning For Fuel Cell Converter With Multiple Sources", in Proc. IEEE Power Electronics Specialist Conf., 2002, pp. 2001-2006.

[12]S. Soter, S. Buchhold, "Adaptable Inverter for Injection of Fuel Cell and Photovoltaic Power", in Proc. IEE Power Conversion Conference, 2002, pp.1453-1455.

[13] P.T. Krein and R. Balog, "Low Cost Inverter Suitable for Medium-Power Fuel Cell Sources", in Proc IEEE Power Electronics Specialist Conference, 2002, pp. 321-326.

[14] Y.R. Novaes and I. Barbi "Low Frequency Ripple Current Elimination in Fuel Cell Systems" digest accepted for the Fuel Cell Seminar - Power Conditioning Systems Special Session. Nov. 2003.

[15] L. A. Serpa, Y. R. Novaes and I. Barbi, "Experimental Parametrization of Steady-state and Dynamic Models Represented by an Electrical Circuit of a PEM Fuel Cell." digest accepted for the COBEP, sept. 2003.